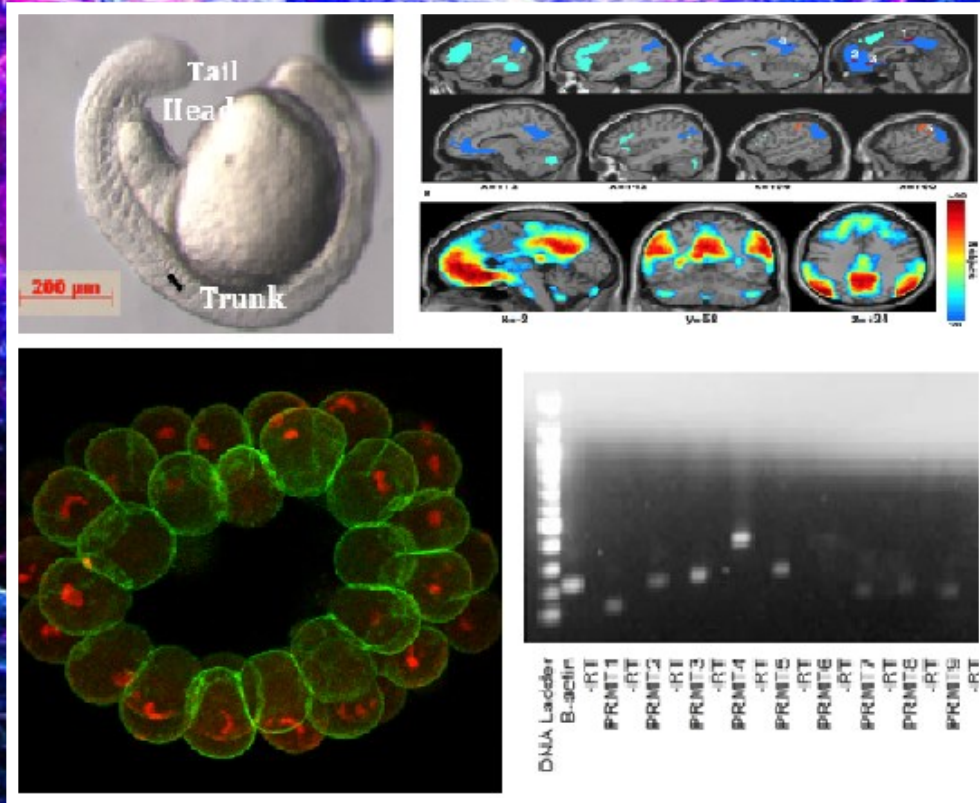


Undergraduate Research Newsletter



University of Miami

Volume 4 Issue 1

June 2015

EDITORS

Faculty Advisor

Prof. Burjor Captain
Department of Chemistry

Student Organizer

Michelle Potiaumpai
Régine Vincent

REVIEW BOARD

Students

Roberto Diaz
Michelle Potiaumpai
Régine Vincent

Faculty

Burjor Captain, Chemistry
Michael Gaines, Biology
Jamie Walls, Chemistry
James Wilson, Chemistry

Special Thanks

Office of Undergraduate Research and Community Outreach

Available Online: For more information please visit the URN homepage under the Office of Undergraduate Research webpage at www.miami.edu

Table of Contents

	Page
Proliferation of Endosteum-derived Mouse Mesenchymal Stem Cells in Hypoxia and Normoxia <i>Berna Buyukozturk</i>	1
Large-scale Brain Network Connectivity in in Attention-Deficit/Hyperactivity Disorder and Autism <i>Rochelle Camino Oliver</i>	4
The Effects of Cdx4 on Zebrafish Somitogenesis <i>Daniel J. Miklin</i>	8
Reliability and Repeatability of Quantitative Tractography Methods for Mapping Structural White Matter Connectivity in Preterm and Term Infants at Term-Equivalent Age <i>Sam Powell</i>	11
The Evolution of 1950s Theater in Miami after the First Major Cuban Exodus <i>Madison Rolls</i>	19
Characterization of Palmitic Acid Methyl Ester: A Novel Vasodilator <i>Stephen Valido and Alexandre do Couto e Silva</i>	21
The Regulation of Gastrulation in the Anthozoan Cnidarian <i>Nematostella vectensis</i> : The Roles of Strabismus and the Cytoskeleton <i>Régine Vincent</i>	24



Foreword

As a teacher, I am elated to see UM undergraduate students generate new results in such a short time to put together a high quality attractive newsletter. This newsletter is an outcome of 'doing' art/science/engineering. My applause and congratulations to the contributing authors who surely will serve as role models for many more UM students to venture into this exciting journey of discovery and innovation through research.

'Doing' something is different from 'reading' about it. The process of doing, be it in science, engineering or art is deeply rewarding in many ways- intellectually, emotionally and socially. Most importantly it gives the much-needed confidence to be successful in life. With the laboratory experience and guidance the students are equipped to make major discoveries in the future.

It is obvious from the life of Michael Faraday, one of the best scientists of the last two centuries, that even a high school diploma is not needed to become a world-renowned scientist. Faraday had no formal education when he started doing experiments and knew no mathematics. His interest in science that motivated him to learn to do experiments on his own eventually led to the discovery of the fundamentals of electromagnetism and the device-dynamo. Events in his life attest to the fact that it is psychologically most important to get results, even if they are not original (in his early days he only repeated the experiments described in books). Making new observations brings with it a great accession of self-confidence and pride. The courage and belief to do important experiments and make meaningful conclusions are avenues to limitless discoveries.

Why should someone undertake such a demanding and challenging path of a researcher in life with a multitude of available easy options? My simple answer is upon looking back one should be proud of how one spent his/her life and be able to tell others that 'I discovered something new, did something that no one else had done before, wrote a novel/book that has generated new thinking, invented a new device that revolutionized the society' etc. To do that one must 'learn, do and communicate' or in the words of Faraday 'work, finish, publish'. The importance of communication in research-based discovery should never be underestimated and that the priority of discovery in science goes to the one who publishes first should not be ignored. It is important to write clearly and concisely and present lucid and cogent formal and informal talks. I am happy to note that the students have done an excellent job of communicating their results in this Newsletter.

To become a researcher of reputation it is important to choose the right problem to solve. The primary aim of research must not be more facts and yet more facts, but more facts of strategic value. Great scientific contributions rarely come from adding another decimal place to known results. In this context getting the 'right' guidance at an early stage as has been provided by various UM faculty to the current authors is of paramount importance. This Newsletter contains beautiful selection of problems in a variety of important disciplines. I hope the students who have participated in the program communicate and share the joy and excitement of doing research to their friends and other young minds and the Newsletter doubles in size in the next year and continues its growth in the future.



V. Ramamurthy
Professor of Chemistry



Proliferation of Endosteum-derived Mouse Mesenchymal Stem Cells in Hypoxia and Normoxia

Berna Buyukozturk (Class of 2015)

Major: Biology

Principle Investigator: Supervisor: Dr. Keith A. Webster & Dr. Roberta Soares

Department: Molecular & Cellular Pharmacology

Supported by Florida Heart Research Institute

Senior thesis: No

Mesenchymal stem cells (MSCs) are adult multipotent cells that can be isolated from the bone marrow. Recent studies have supported that regional hypoxia in the bone marrow may play a role in regulating stem cell proliferation, survival, metabolism, paracrine effects, and multipotency. MSCs from the endosteum are exposed to lower levels of oxygen than MSCs from vascular niches. Scientists are investigating strategies such as hypoxic preconditioning to increase successful engrafting of MSCs during stem cell therapy for ischemic diseases such as coronary heart disease and atherosclerosis. We propose that hypoxia increases the proliferation capacity of endosteal MSCs, and that these cells might present unique features and capacity when isolated and expanded under conditions that mimic their naturally hypoxic microenvironment. Our experiment using mMSCs from the vascular niches is currently in progress. Our results show that the average proliferation rate for endosteal mMSCs was significantly greater in hypoxia than in normoxia.

Studies have shown that MSCs can express phenotypic characteristics of endothelial, neural, smooth muscle, skeletal myoblasts, and cardiac myocytes and can prevent deleterious remodeling and improve recovery when introduced into the infarcted

heart.¹⁻³ MSCs are remarkable in their ability to migrate to damaged tissue or sites of inflammation, and to secrete a variety of angiogenic cytokines.² MSCs from the thin outer layer of the bone marrow, called the endosteum, are exposed to lower levels of oxygen than MSCs from the inner vascular niches.^{1, 4-6} The MSCs in the vascular niches are provided with greater exposure to oxygenated blood and they have been studied for the past two decades.^{1, 5, 6}

For this proposed project, I compared the proliferation rates of endosteal mouse mesenchymal stem cells (mMSCs) in normoxic versus hypoxic conditions. The mMSCs were isolated from murine bone marrow of the femur and tibia, and cultured in media until passage seven. One set of cells were grown and passaged in 21% oxygen (normoxia) and the other in 2% oxygen (hypoxia). The same number of normoxia endosteum-derived mMSCs (1.5×10^4) was plated in triplicate wells, to grow over a period of seven days without passage and only changing the media. A different triplicate set was trypsinized and counted on day 2, day 4, and day 7. The same will be done simultaneously for the endosteum-derived cells in hypoxic conditions. We achieved the condition of hypoxia by using a hypoxia chamber set to 2% O₂ (it is important to note however that the O₂ in the endosteum can be <2%), where the cells had been plated since their isolation.

Our results so far show that the average proliferation rate for endosteal mMSCs was significantly greater in hypoxia than normoxia. For day 4 through day 7, specifically, the average growth rate of



endosteal mMSCs in hypoxia was more than 3 times greater when compared to normoxia conditions ($p < 0.02$) (Figures 1 & 2). This suggests that conditioning these cells in an environment of oxygen tension that mimics their natural microenvironment in the body may be useful in further studies of hypoxic preconditioning of MSC engraftments and stem cell therapies for ischemic diseases.

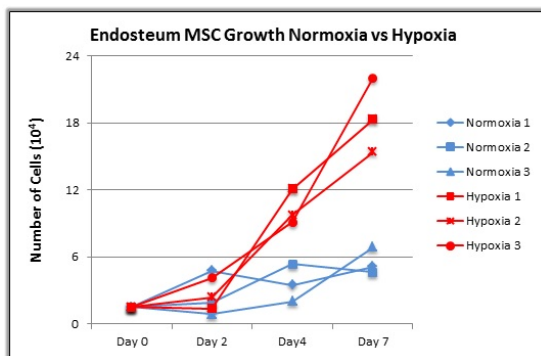


Figure 1. The cell counts on days 0, 2, 4, and 7 for each well.

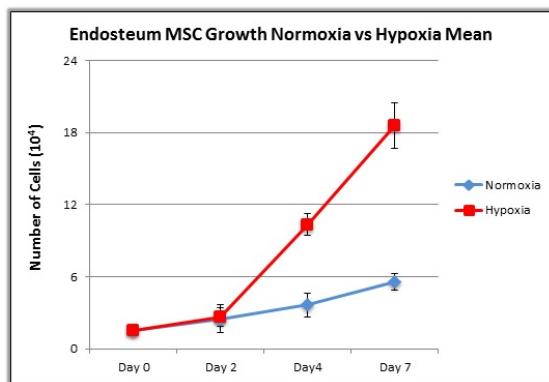


Figure 2. The averages of cell counts on days 0, 2, 4, and 7 for each triplicate.

The same experimental design is currently in progress for the isolated vascular mMSCs. We would like to repeat the same experimental design using using 5% O₂ instead of 21% O₂, to mimic physiological conditions. Further investigation of these cells would require flow cytometry characterization of the mMSCs by testing positive for specific mMSC surface markers CD105, CD73, CD90, and Sca-1, and negative for CD45, CD31, CD11b, and CD34. Testing positive or negative for these surface proteins will help us identify the cell population. Additionally, we are interested in comparing levels of expression of c-kit marker, a cell surface protein commonly associated with stem cells, for the cells in normoxia and hypoxia in order to investigate whether hypoxia affects stem phenotype enrichment.

Cardiovascular disease is one of the leading causes of mortality and morbidity worldwide. Improving the survival skill of MSCs to engraft in a hostile injured environment is important for increasing the efficacy of stem cell therapy. We believe that MSCs that reside in the severely hypoxic endosteal niche might present unique features and capacity when isolated and expanded under conditions that mimic their naturally hypoxic microenvironment. If so, strategies such as hypoxic preconditioning MSCs for engrafting in stem cell therapy could improve rates of success, and aid the recovery of living tissue. Our goal is to also contribute to the growing data on MSC surface antigen expression, and assess the potential differences in c-kit positive cells in normoxia



and in hypoxia as it relates to how oxygen levels regulate the stem profile.

References

- [1] V. A. Siclari et al (2013) Mesenchymal progenitors residing close to the bone surface are functionally distinct from those in the bone marrow. Elsevier: Bone 53:575-586.
- [2] M. F. Pittenger et al (2004) Mesenchymal Stem Cells and Their Potential as Cardiac Therapeutics. American Heart Association 95:9-20.
- [3] F. P. Barry 2003) Biology and Clinical Applications of Mesenchymal Stem Cells. Birth Defects Research (Part C) 69:250-256.
- [4] K. Parmar et al (2007) Distribution of hematopoietic stem cells in the bone marrow according to regional hypoxia. PNAS 104(13):5431-5436.
- [5] I. G. Winkler, et al (2010) Positioning of bone marrow hematopoietic and stromal cells relative to blood flow in vivo: serially reconstituting hematopoietic stem cells reside in distinct nonperfused niches. Blood 116(3):375-385.
- [6] M. J. Kiel et al (2006) Maintaining Hematopoietic Stem Cells in the Vascular Niche. Immunity 25(6):862-864.
- [7] H. Kubo et al (2009) c-Kit⁺ Bone Marrow Stem Cells Differentiate into Functional Cardiac Myocytes. Clinical and Translational Science. 2(1):26-32.



Large-scale Brain Network Connectivity in Attention-Deficit/Hyperactivity Disorder and Autism

Rochelle Camino Oliver (Class of 2015)

Major: Biomedical Engineering/ Premed concentration track

Principal Investigator/Supervisor: Dr. Jason Nomi and Dr. Lucina Uddin

Department: Psychology/Neurology

Fellowship/Awards/Recognition: Presented at 23rd

Annual University of Miami/Jackson Hospital

Neuroscience Research Day 2014

Senior Thesis: No

Attention-deficit/hyperactivity disorder (ADHD) is diagnosed in approximately 1 out of every 10 children, while autism spectrum disorder (ASD) is diagnosed in approximately 1 out of every 68 children (CDC). Previous research has shown that children with ADHD generally exhibit hypo-connectivity (Posner et al., 2014) while children with ASD generally show hyper-connectivity (Uddin et al., 2013a, 2013b) of large-scale brain networks when compared with typically developing (TD) children. The current study explored whole-brain functional connectivity in children with ADHD, ASD, and TD children in order to compare how functional connectivity differs across these three groups.

This study examined how functional connectivity of large-scale brain networks is represented in ADHD and autistic populations by using a dual regression independent component analysis. This type of analysis has previously shown that individuals with ADHD typically have under-connected large scale brain networks compared to normal controls while individuals with autism typically have over-connected large scale brain networks

compared to normal individuals. However, no study has directly compared all three populations within the same analysis.

In order to perform this experiment, a functional MRI was used in order to detect resting state functional connectivity. Resting state functional connectivity concentrates on connectivity among time points during resting conditions. MRI with functional connectivity may be a key factor to future analysis of mental disorders and evaluation of treatment in the medical and research fields. Functional connectivity changes with respect to time and consists of high level cognitive function. Through investigating functional connectivity, brain networks were observed such as the Default Mode Network. The Default Mode Network (DMN) is a network of brain regions that are active when an individual is at rest and awake. This network is particularly activated when participants focus on tasks such as daydreaming, and retrieving memories. It is indirectly correlated with brain networks that focus on external visual signals. The DMN is highly studied because it is one of the most easily visualized brain networks. Other resting state networks also known as “components” have been functionally correlated with resting state. Such components are: sensory/motor component, executive control component, visual component, frontal/parietal component, temporal component, etc. These components although largely separated share a high signal activity known as the “Blood-oxygen-level dependent” (BOLD) signal. BOLD signals display the levels of blood flow that occur in different regions throughout brain networks



that are known to share and support cognitive functions.

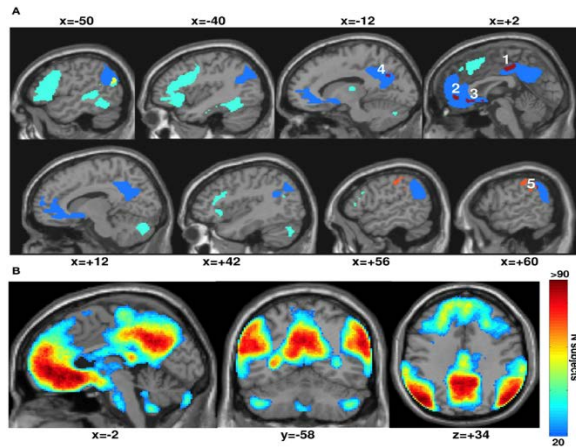


Figure 1. fMRI images of a subject's Default Mode Network (DMN).

In order to obtain data and information of each component, a series of programs were ran with Linux and FSL which is a library of analysis tools used for fMRI and MRI imaging data. To further organize the three research groups, the resting state functional MRI data was collected from 57 children of ages 6-12 obtained from the publicly available ABIDE (http://fcon_1000.projects.nitrc.org/indi/abide/) and ADHD-200 (http://fcon_1000.projects.nitrc.org/indi/adhd200/) datasets. Three groups were organized with 19 subjects in each. The following groups were: ADHD versus TD; ASD versus TD; and ADHD versus ASD versus TD. As previously mentioned, subjects were observed under resting state, or lack of task and activity. Resting state fMRI can be used to evaluate brain region interactions that occur when a subject is lacking of an activity or task. Through these collected BOLD signals subjects were analyzed through

Independent Component Analysis (ICA). ICA is a useful statistical approach in the detection of resting state networks by separating a signal to spatial and time components. With ICA, the subjects' images are facilitated with the removal of noise of signals and has been a reliable extract of default mode network. After running an ICA for resting-state fMRI, series of images displayed high and low functionally connected networks between the three testing groups.

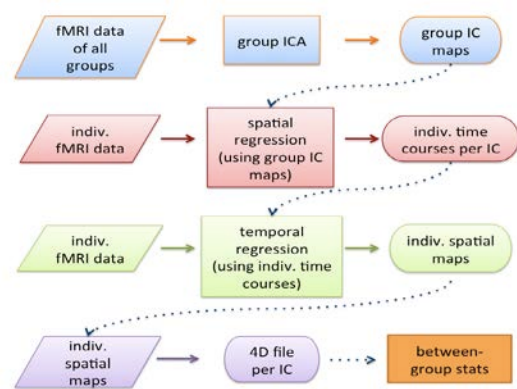


Figure 2. Description of process of collecting data, interpretation, and dual regression analysis using FSL view.

A group average ICA was estimated and a version of each group level spatial maps was obtained using a dual regression analysis. To summarize, a dual regression independent component analysis consists of three steps. First, large-scale functional brain networks called "independent components" are identified for all individuals. Second, individual representations of these independent components are acquired for each individual. Finally, statistical testing is used to determine if differences in functional



connectivity exist between groups. Then, spatial maps were compared to observe differences in the groups of subjects using a permutation test to analyze statistical significance as shown in the table below.

Children (6-12)	ASD	TD	ADHD	P Value
Mean Age	9.51(1.12)	9.18(1.18)	9.09(1.47)	0.536
Age Range	7.15-10.96	8.01-10.86	7.35-11.72	
Gender	18M/1F	12M/7F	13M/6F	
Full IQ	107.77(16.16) (76-142)	113.04(13.67) (80-136)	103.12(12.27)(81-120)	0.134
ADI Social Score	19.6(5.86) (7-27)			
ADI Verbal Score	16.11(3.80) (8-22)			
ADI RRB	5.67(2.25) (3-10)			
ADOS Communication	3.26(1.76)(0-7)			
ADOS Social	7.72(2.96) (4-14)			

Figure 3. Permutation Test using the mean scores of ADHD, ASD, and TD subjects.

The results confirm that individuals with ADHD have less functional connectivity than normal controls while individuals with ASD have more functional connectivity than normal controls. However, the three-group analysis showed that individuals with ADHD had less functional connectivity than normal controls with no differences for the ASD group.

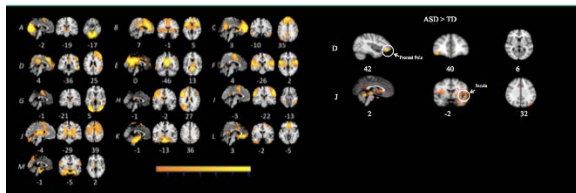


Figure 4. Group of subjects comparison between ASD and TD groups. ASD subjects are hyper-connected compared to normal subjects.

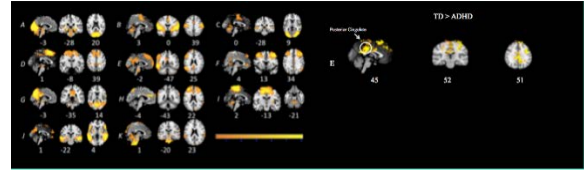


Figure 5. Group of subjects comparison between ADHD and TD groups (shown above). ADHD patients are shown to be hypo-connected compared to normal subjects.

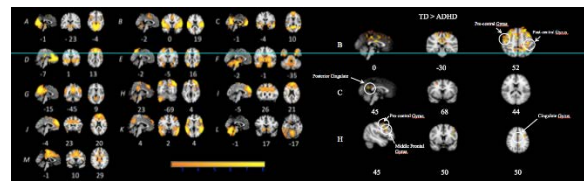


Figure 6. Group of homogenous subjects comparison between ASD, ADHD, and TD subjects. ADHD patients were confirmed to be hypo-connected compared to TD patients.

Therefore, this collection of data highlights functional signatures of the two most prevalent neurodevelopmental disorders. For future research, a few changes should be adjusted in order to gain further insight in regard to the overall three group category. The most important suggestions would be to have a greater subject pool for the study and to further gather more homogenous subjects within each category. For the category of ADHD participants, the subjects had more heterogeneity (ethnicity, race, age) compared to ASD subject group. Using fMRI and functional connectivity measures and methods can expand the neuroscience field as scientists continue to understand and study brain disorders by comparing such populations to typically developing groups.



References

- [1] Posner, J., Park, C., Wang, Z. (2014). Connecting the dots: A review of resting connectivity MRI studies in attention-deficit/hyperactivity disorder. *Neuropsychology Review*, 24, 3-15.
- [2] Uddin, L.Q., Supekar, K., Menon, V. (2013). Reconceptualizing functional brain connectivity in autism from a developmental perspective. *Frontiers in Human Neuroscience*, 7:458.
- [3] Uddin, L.Q., Supekar, K., Lynch, C., Khouzam, A., Phillips, J., Feinstein, C., Ryali, S., & Menon, V. (2013). Salience network based classification and prediction of symptom severity in children with autism. *JAMA Psychiatry*, 70(8), 869-879.



The Effects of Cdx4 on Zebrafish Somitogenesis

Daniel J. Miklin (Class of 2015)

Major: Microbiology and Immunology
Principal Investigator/Supervisor: Dr. Isaac Skromne
Department: Developmental Biology
Senior Thesis: No

Vertebrae of the spinal column originate from embryonic somites through complex processes involving the activity of numerous genes. Among these genes, the Hox family of transcription factors has been shown to be critical for somite anterior-posterior identity. Hox expression is partially regulated by the Cdx family of transcription factors. Loss of Cdx results in posterior body truncation as well as shifts and down-regulation in Hox gene expression. However Cdx activity in somite morphogenesis is unknown. Taking a gain of function approach, we investigated the effect of Cdx4 on somite formation. A transgenic line of zebrafish carrying an inducible Cdx4 gene was activated to express Cdx4 at the tailbud stage. We found that at the 18-somite stage, the lengths of the somites formed at the time of heat shock were different than the control. We conclude that the presence of Cdx4 during somitogenesis has a direct effect upon limiting somite growth and size.

Vertebrae are regular structures that form from similar repeating units that collectively form the spinal column in vertebrates. Each of the vertebrae originates from a group of mesodermal cells that form a cluster called somites (Dequéant and Pourquié, 2008). Somitogenesis is the process of developing somites. These structures are evolutionarily conserved across vertebrates (Dequéant and Pourquié, 2008). Somites all form in the same manner,

but due to their identity they can differ in size. The source of these variations lies in the processes that generate and bestow identity to somites. This action is performed by a set of regulatory genes known as Hox genes.

The homeobox, or Hox, gene family is a group of regulatory genes that encode transcription factors that regulate patterning during ontogenesis (Burke et al. 1995). These genes help determine the segmental identity of each vertebrae. They are regulated by several signaling factors (Shimizu et al. 2006). The most important signaling factor in Hox regulation and somitogenesis is fibroblast growth factor (FGF). FGF directly regulates somitogenesis and somite identity by specifying which area of the paraxial mesoderm is competent to begin segmenting (Keenan et al. 2006). However, the identity of the transcription factors that FGF regulates to promote or prevent tissue segmentation remain unknown. We hypothesize that FGF regulates somitogenesis through the transcriptional control of Cdx, a gene that is regulated by FGF during process of identity specification (Lin & Slack 2008). In preliminary data from our lab, Cdx4 mutants have been shown to display a reduction in somite size, suggesting that Cdx could be the regulatory link between somitogenesis and somite identity.

We used a gain of function approach to look at the effects of Cdx4 on somite formation. To measure these effects we overexpressed Cdx4 from a transgene ectopically, and measured variation in somite length in embryos at the 18-somite stage. This data was then compared to wild type somite length to determine significance. Our



results indicate that Cdx4 may have a significant effect on somite size.

In order to examine the effect of Cdx4 on somite formation, the transcription of the Cdx4 gene needed to be temporally induced. To accomplish this, a transgenic line containing a heat shock promoter for the Cdx4 gene was used (Skromne et al. 2007). Heat shock proteins are expressed when exposed to higher temperatures. Therefore expression of the Cdx4 gene can be controlled by manipulating the temperature. At higher temperatures the transgene becomes activated and Cdx4 is transcribed.

Embryos were exposed to an increase in temperature at the tailbud stage for one hour to activate the heat shock promoter. To ensure that the temperature was not causing non-specific effects, the wild type controls were exposed to the same changes in temperature. Upon reaching the 18-somite stage the embryos were dechorionated and imaged. The images were then processed, and the distance between somite was measured based on the ratio of 1 pixel:1 μm (Fig 1).

When comparing individual somites between wild type and transgenic embryos, the average length of each somite varied by 5 μm or less, a non-significant difference for most somites (Fig. 2). The only significant differences in length occurred at somite 1 and somite 10. At these somites the size of the transgenic somites was significantly smaller than in the wild type (Fig. 2). At somite 1 the average length in wild type embryos was 52.101 μm , compared to 42.414 μm in the transgenic embryos. At somite 10, the average length in the wild type was 53.911

μm compared to 46.421 μm in transgenic embryos. Given that at the time of Cdx4 transgene induction, somite 1 is segmenting and the tissue for somite 10 is being incorporated into the axis, these results suggest that Cdx4 may have an important function in regulating somitogenesis. This result will need to be confirmed in future work.

Figure 1. Representative wild type zebrafish embryo



at 20-somite stage indicating the position of somites. The head, trunk and tail are indicated. Line indicates one somite length. Scale bar, 200 μm .

We predicted a significant difference in somites 10-18 because the heat shock was performed at the tailbud stage, when the tissue that will form the 10th somite is being generated. Our hypothesis was that Cdx4 would affect the size of the somites that were formed post-heat shock. The results showed that the wild type somites were significantly larger at somites 1 and 10. These results are in partial agreement with our hypothesis, as indeed somite 10 was affected. However, it does not explain how the process is regulated,



nor the mechanism by which *Cdx4* changed somite size.

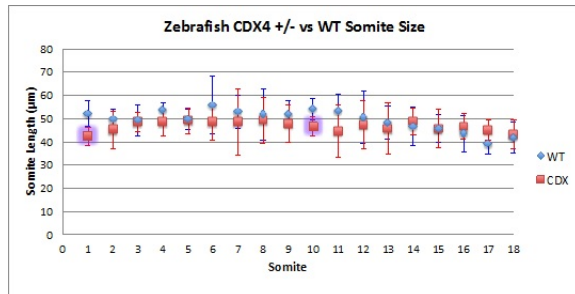


Figure 2. Somite size variation for the first 18 somites in wild type and transgenic embryos induced to express *Cdx4* (in μm). The wild type data points are shown in blue and the transgenic data points in red. Statistically significant data points are highlighted in purple (*Cdx4* vs. wt for somite 1 $p \leq 0.0156$ and for somite 10 $p \leq 0.0291$).

One possible explanation for the changes in somite 1 and 10 lies in the somitogenic activity of FGF. Experimental evidence supports a model in which FGF regulates *Cdx4* transcription to bestow axial identity to somite precursor cells. The transcriptional domain of FGF and *Cdx4* overlap in the non-somitogenic region of the paraxial mesoderm. Based on the inhibitory activity that *Cdx4* has on somitogenesis, we propose that the region in which both FGF and *Cdx4* molecules overlap, somitogenesis is blocked. Therefore, in these areas where FGF and *Cdx4* are no longer transcribed, the tissue can segment into somites. Under this model, when the levels of *Cdx4* are artificially increased, *Cdx4* protein would prevent somitogenesis, thus generating smaller somites.

While the experiment indicates a potential involvement of *Cdx4* in the regulation of somite size, these results do not

provide any insight into the mechanism by which somite formation is blocked. It is unclear whether *Cdx4* works alone, or in conjunction with FGF to block somitogenesis. To address this issue an experiment should be performed in which FGF is overexpressed. Whether or not the overexpression leads to a decrease in somite size will indicate whether FGF helps in the blocking process, or only acts as a regulatory molecule for *Cdx4*.

References

- [1] A. C. Burke, C. E. Nelson, B. A. Morgan, C. Tabin. "Hox Genes and the Evolution of Vertebrate Axial Morphology." *Development* 121 (1995): 333-46.
- [2] M-L Dequéant, O. Pourquié. "Segmental Patterning of the Vertebrate Embryonic Axis." *Nature Reviews Genetics* 9.5 (2008): 370-82.
- [3] I. D. Keenan, R. M. Sharrard, H. V. Isaacs. "FGF Signal Transduction and the Regulation of *Cdx* Gene Expression." *Developmental Biology* 299.2 (2006): 478-88.
- [4] G. Lin, J. Slack. "Requirement for Wnt and FGF Signaling in *Xenopus* Tadpole Tail Regeneration." *Developmental Biology* 319.2 (2008): 558.
- [5] T. Shimizu, Y.-K. Bae, M. Hibi. "Cdx-Hox Code Controls Competence for Responding to Fgfs and Retinoic Acid in Zebrafish Neural Tissue." *Development* 133.23 (2006): 4709- 719.
- [6] I. Skromne, D. Thorsen, M. Hale, V. E. Prince, R. K. Ho. "Repression of the Hindbrain Developmental Program by *Cdx* Factors Is Required for the Specification of the Vertebrate Spinal Cord." *Development* 134.11 (2007): 2147-15.



Reliability and Repeatability of Quantitative Tractography Methods for Mapping Structural White Matter Connectivity in Preterm and Term Infants at Term-Equivalent Age

Sam Powell (Class of 2015)

Major: Neuroscience, 2015

Principle Investigator/Supervisor: Nehal A. Parikh, D.O., M.S.

Department: Center for Perinatal Research, The Research Institute at Nationwide Children's Hospital; Department of Neurosciences, The Ohio State University

Senior Thesis: No

Premature infants exhibit widespread insults and delays in white matter maturation that can be sensitively detected early using diffusion tensor imaging (DTI). Diffusion tensor tractography (DTT) facilitates in vivo visualization of white matter tracts and has the potential to be more sensitive than simpler two-dimensional DTI-based measurements. However, the reliability and reproducibility of performing tractography for major white matter tracts in preterm infants is not known. The main objective of our study was to develop highly reliable and repeatable methods for ten white matter tracts in extremely low birth weight infants (ELBW, birth weights ≤ 1000 g) at term-equivalent age. To demonstrate clinical utility, we also compared fiber microstructural and macrostructural parameters between preterm and healthy term controls. Twenty-nine ELBW infants and a control group of 15 healthy term newborns were studied. A team of researchers experienced in neuroanatomy/neuroimaging established the manual segmentation protocol based on a priori anatomical knowledge and an extensive training period to identify sources of variability. Intra- and inter-rater reliability and repeatability were

tested using intra-class correlation coefficient within-subject standard deviation (SD), repeatability, and Dice similarity index. Our results support our primary goal of developing highly reliable and reproducible comprehensive methods for manual segmentation of 10 white matter tracts in ELBW infants. The within-subject SD was within 1–2% and with repeatability within 3–7% of the mean values for all 10 tracts. The intra-rater Dice index was excellent with a range of 0.97 to 0.99, while the inter-rater Dice index was lower (range: 0.80 to 0.91) but still within a very good reliability range. ELBW infants exhibited fewer fiber numbers and/or abnormal microstructure in a majority of the ten quantified tracts, consistent with injury/delayed development. This protocol could serve as a valuable tool for prompt evaluation of the impact of neuroprotective therapies and as a prognostic biomarker for neurodevelopmental impairments.

Diffusion tensor tractography (DTT), a three-dimensional diffusion tensor imaging (DTI) technique, is now evolving into a potent investigative tool to study early brain development and white matter structural connectivity in vivo. Diffusion parameters such as fractional anisotropy (FA) and diffusion coefficients, such as mean diffusion (MD), axial diffusivity (AD), and radial diffusivity (RD), provide vital insights into the degree of myelination and white matter organization.¹⁻³. The degree of diffusion within the developing human brain is influenced by many critical factors such as relative membrane permeability of water, tissue water content, degree of myelination and the dense packing of axons. Its application in very preterm infants has the potential to enhance our understanding of the encephalopathy of prematurity that is heavily



affected by preoligodendrocyte and axonal injury and aberrant white matter development.^{3,4}

Recent studies have made significant progress in mapping detailed human adult brain anatomy of white matter tracts and their connectivity using DTT.^{1,2, 5-7} Furthermore, tractography results of major white matter fibers obtained from these adult studies were reported to be in agreement with classical definitions based on postmortem studies.⁶ To a lesser degree, DTT has also been used to study neonatal brain development and white matter connectivity. Preliminary studies in preterm infants have explored white matter density and fiber maturation in developing brains.⁸⁻¹⁴ However, there are significant challenges in studying neonatal white matter brain anatomy and connectivity. The developing neonatal brain has very different tissue characteristics compared to adult brains, such as the degree of myelination and water content, resulting in lower FA values in the white matter tracts.¹⁴ Neonatal scans also have lower image contrast due to incomplete myelination, lower signal-to noise ratio resulting from a need for shorter scan times, and lower spatial resolution due to smaller head size.¹⁴ Recent investigators have demonstrated the feasibility of performing white matter tractography in preterm infants.^{15,16} Additional clinical studies suggest that white matter tract development is adversely affected by premature birth¹⁷⁻¹⁹ and that measures of tract diffusion and/or length are promising independent predictors of neurodevelopmental impairments²⁰⁻²¹. Yet, only a few tracts have been studied, and tractography methodology has not been

sufficiently tested for reliability or repeatability in very preterm infants.

The main objective of our study was to develop highly reliable and reproducible methods for manual segmentation of ten well-delineated white matter tracts in extremely low birth weight (ELBW; BW ≤ 1000 g) infants at term-equivalent age. The feasibility of tractography of these ten white matter tracts could serve as a prognostic biomarker for neurodevelopmental impairments in preterm infants. A secondary objective was to compare tract-based parameters between healthy term control infants and ELBW infants. The following ten white matter tracts were categorically segmented and classified: (I) *Commissure fiber tract*: corpus callosum (CC); (II) *Projection fibers*: corticospinal fiber tract (CST); (III) *Association tracts*: inferior longitudinal fasciculus (ILF), inferior-fronto occipital (IFO) tract, and the uncinate fasciculus (UNC) bundle; (IV) *Limbic system tracts*: cingulum in the cingulate gyrus (CG) and the fornix (FX) fiber bundle; (V) *Visual cortex tract*: Optic radiations (OR); (VI) *Cerebral peduncles*: middle cerebellar peduncle (MCP) and superior cerebellar peduncle (SCP).

Subjects

Based on an assessment of image quality and signal abnormalities such as subject motion and geometric distortions, a study population of 29 ELBW infants was randomly chosen from an imaging cohort of 50 ELBW infants. All infants were cared for in the Children's Memorial Hermann Hospital NICU from May 2007 to July 2009.



Infants with severe white matter injury or any major congenital anomalies were excluded. A control group of 16 healthy, 1- to 4-day old full-term newborns (37 to 41 weeks appropriate for gestational age) from the well-baby nursery were also selected. All infants were appropriate for gestational age and were excluded if they had any history of perinatal distress or complications (see 2, for additional details). One term infant was excluded for severe motion artifacts that interfered with tract segmentation.

MRI Acquisition

All subjects were transported to the MRI scanner and supervised during scanning by three experienced neonatal personnel – a transport nurse, a research nurse, and a neonatologist. All MRI scans were performed during natural sleep, without sedation, after infants were fed, swaddled, and restrained in a transporter, MedVac Infant Vacuum Splint (CFI Medical Solutions, Fenton, MI). MRI noise was attenuated using Insta-Puffy Silicone Earplugs (E.A.R. Inc, Boulder, CO) and Natus Mini Muffs (Natus Medical Inc, San Carlos, CA). The MRI scans were performed on a 3T scanner (Achieva, Philips Medical Systems, Best, Netherlands), which was equipped with a 32 channel receiver and a gradient system, capable of producing gradient amplitudes of 80mT/m with a slew rate of 200 T/m/s. A head coil of 8-channel phased array was used for data acquisition purpose. The study DTI protocol comprised of a single-shot, spin-echo planar sequence with TR/TE, 6000/61; in plane resolution 1.6×1.6 mm², field of view (FOV), 180 mm²; 112×112 matrix; and 2-mm continuous

slices. 15 directions of diffusion gradients were used with a b value of 800 s/mm², and another image with no diffusion gradient was obtained (b = 0 s/mm²).

Image Processing

The DTI data was transferred to a PC with Windows platform and processed using DTI Studio (software developed by H. Jiang and S. Mori, Johns Hopkins University). FSL software (developed by the Analysis Group, FMRIB, Oxford, UK) was used for eddy current correction using the B0 image, which corrects for imaging artifacts and subject motion. Then we aligned the mean diffusion-weighted images using a 12-point affine AIR program in DTI Studio to remove any small bulk motions that occur during scanning. The lead author then inspected all images for possible artifacts due to infant motion or scanner malfunction. The six elements of the diffusion tensor were calculated for each pixel in DTI Studio. The tractography tool in DTI Studio is based on the Fiber Assignment by Continuous Tracking (FACT) method and brute-force approach, which performs the tracking from all the pixels within the brain^{22, 23-25}. The eigenvector associated with the largest eigenvalue was used to determine fiber orientation. This method required a specific FA threshold and fiber tracking angle for each fiber tract during segmentation. A multiple ROI seed selection approach was utilized for the 3D white matter tract reconstruction based on existing prior anatomical knowledge of the white matter fiber trajectories. In the multi-ROI approach, three types of functional operations – “OR”, “AND” and “NOT” – were used depending upon the fiber tract trajectory. Because we



wished to reproduce full tracts, the “CUT” operation, which restricts tracts between two ROIs, was not used. The OR operation was used to select the fibers passing through either specific ROI-A or ROI-B. It was primarily used to define the first ROI for all the white matter tracts. The AND operation was used to restrict or filter the fibers which penetrate or were common to both ROI-A and ROI-B with known prior knowledge, but also included fibers before ROI-A and after ROI-B. Last, the NOT operation was used to remove extraneous fiber projections which did not belong to the actual fiber trajectory of a desired fiber tract bundle. We used color-coded maps, fractional anisotropy, and trace maps to locate landmarks for segmenting the white matter tracts.²⁶

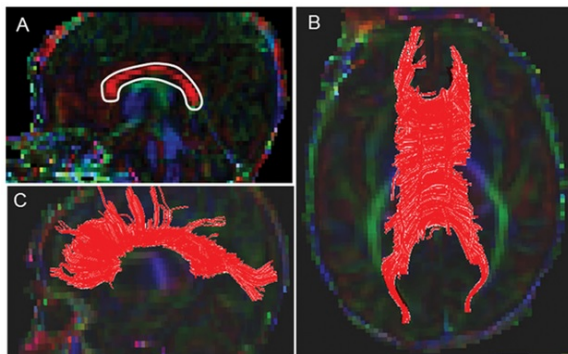


Figure 1. Location of single ROI on DTI color maps for the corpus callosum (CC) in a preterm infant.

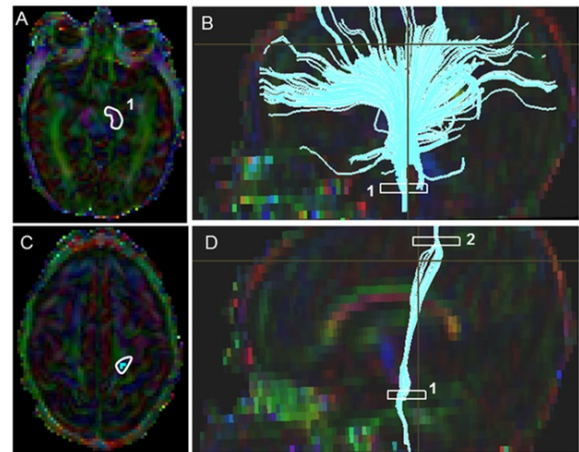


Figure 2. Location of ROIs on DTI color maps for the corticospinal tract (CST) in a preterm infant.

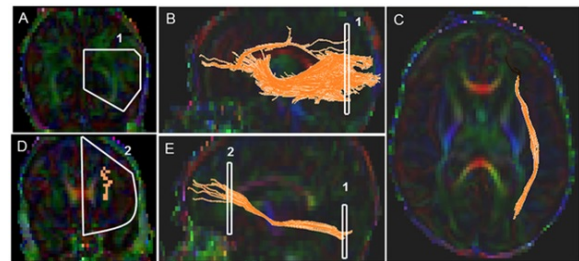


Figure 3. Location of ROIs on DTI color maps for the inferior fronto-occipital (IFO) tract in a preterm infant.

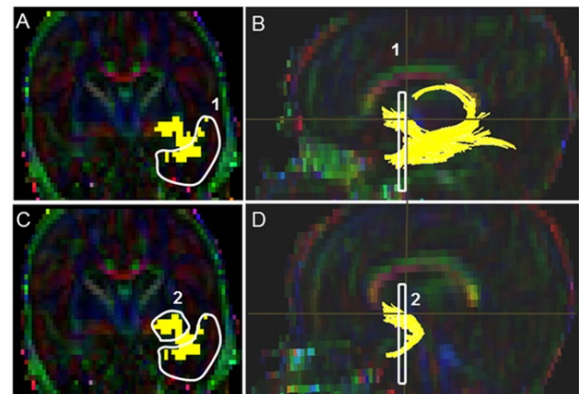


Figure 4. Location of ROIs on DTI color maps for the uncinate (UNC) tract in a preterm infant.

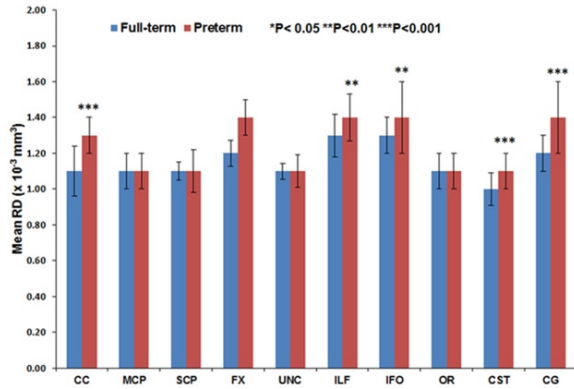


Figure 5. Mean RD for ten major white matter tracts in healthy term controls (blue bars) and ELBW infants (red bars).

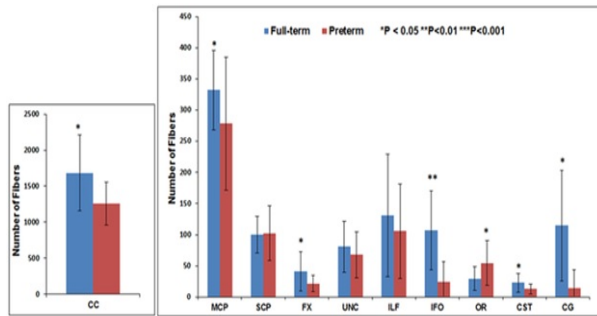


Figure 6. Mean number of fibers for ten major white matter tracts in healthy term controls (blue bars) and ELBW infants (red bars).

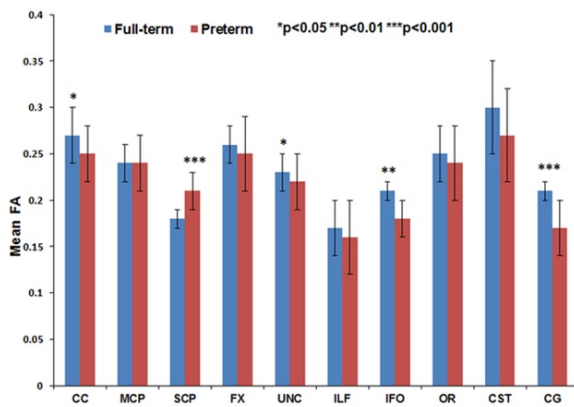


Figure 7. Mean fractional anisotropy for ten major white matter tracts in healthy term controls (blue bars) and ELBW infants (red bars).

Tract	Mean (SD)	With-subject SD	Repeatability	ICC (95% CI)
MCP	1194.2 (350.4)	13.5	37.3	0.998 (0.989, 0.999)
SCP	398.9 (118.8)	6.2	17.2	0.996 (0.995, 0.999)
CC	3803.4 (1153.4)	18.6	51.5	0.995 (0.993, 0.998)
FX	233.1 (77.5)	5.4	14.8	0.978 (0.967, 0.992)
CG	353.4 (271.9)	5.6	15.4	0.985 (0.980, 0.989)
CST	180.3 (71.0)	1.8	5.1	0.997 (0.994, 0.999)
OR	281.9 (98.8)	3.9	10.9	0.981 (0.971, 0.996)
UNC	226.7 (108.7)	3.8	10.4	0.997 (0.996, 0.998)
IFO	564.9 (365.5)	4.3	11.9	0.988 (0.989, 0.999)
ILF	626.2 (345.3)	16.3	45.3	0.998 (0.997, 0.999)

doi:10.1371/journal.pone.0085807.t001

Table 1. Mean total number of voxels with corresponding intra-rater measurement error, repeatability coefficient, and reliability data for ten white matter tracts in preterm and term infants.

In this study we presented a comprehensive and highly reliable neonatal protocol for deterministic tractography for ten white matter tracts. We were also able to demonstrate high intra-rater and inter-rater repeatability after two raters repeated measurements in all 44 subjects. The intra-rater Dice index was excellent, within a range of 0.97 to 0.99, the inter-rater Dice index was lower (range: 0.82 to 0.91), but still within a very good reliability range. These results support our primary objective of developing a comprehensive, reliable and reproducible approach to neonatal tractography, suitable for further use in large randomized clinical trials or population-based studies.

The group differences we observed between ELBW and healthy term infants in



FA, MD, number of fibers and number of voxels also confirm the validity of our measures. As expected for many of the tracts, the full-term control group exhibited greater fiber numbers, fiber volume, and mean FA values and lower MD as compared to ELBW infants, with up to five tracts exhibiting significant differences.

The high reliability and repeatability metrics for ten major white matter tracts was a major strength of our study. This was facilitated by our use of an extensive training period and a multiple ROI approach that was based on neuroanatomical knowledge from adult studies. Marked group differences between preterm and term infants in tract micro and macrostructure provided further evidence that our approach is clinically useful. However, some limitations involved with tractography techniques deserve mention. The results are dependent upon the quality of the DTI image acquisition, including spatial resolution, signal-to-noise ratio, and motion artifacts and the image pre-processing algorithm used. Tractography measures such as fiber number are semi-quantitative at best, and have not been validated with postmortem studies. Nevertheless, they may offer another useful measure of tract integrity in individual patients or to compare different groups of subjects.

Diffusion measures such as FA and MD are well accepted to provide a useful characterization of white matter microstructural development. In extremely preterm infants, emerging studies suggest they are associated with perinatal interventions and neurodevelopmental

impairments.²⁷⁻²⁹ Use of full tract based measures of microstructure and macrostructure as compared to ROI-based measures should prove more robust in the diagnosis of injury/delay and prediction of outcomes. Advanced MRI measures such as DTT are more sensitive than current neonatal imaging measures and when combined, could prove to be a valuable surrogate endpoint for neurodevelopmental outcomes. In particular, earlier knowledge of cognitive impairment risk, which cannot be accurately diagnosed until 5 years of age, holds the greatest potential for benefitting preterm infants.³⁰

We demonstrated development of highly reliable and reproducible comprehensive methods for manual segmentation of important white matter tracts in ELBW and term neonates. Extremely preterm infants exhibited fewer fiber numbers and reduced volume and/or abnormal microstructure in a good majority of the white matter tracts studied, such as CC, IFO, CG, CST, MCP, and FX. These results were consistent with delayed white matter development and/or injury.³¹⁻³³ This protocol could serve as a valuable tool for prompt evaluation of the impact of neuroprotective therapies and as a prognostic biomarker for neurodevelopmental impairments.³⁴

References

- [1] Basser PJ, Mattiello J, LeBihan D (1994) MR diffusion tensor spectroscopy and imaging. *Biophys J* 66: 259–267.
- [2] Basser PJ, Pajevic S, Pierpaoli C, Duda J, Aldroubi A (2000) In vivo fiber tractography using DT-MRI data. *Magn Reson Med* 44: 625–632.
- [3] Le Bihan D, Mangin JF, Poupon C, Clark CA, Pappata S, et al. (2001) Diffusion tensor imaging: Concepts and applications. *J Magn Reson Imaging* 13: 534–546.



- [4] Volpe JJ (2009) Brain injury in premature infants: a complex amalgam of destructive and developmental disturbances. *Lancet Neurol* 8: 110–124.
- [5] Ment LR, Hirtz D, Huppi PS (2009) Imaging biomarkers of outcome in the developing preterm brain. *Lancet Neurol* 8: 1042–1055.
- [6] Catani M, Howard RJ, Pajevic S, Jones DK (2002) Virtual in vivo interactive dissection of white matter fasciculi in the human brain. *Neuroimage* 17: 77–94.
- [7] Catani M, Jones DK, Donato R, Ffytche DH (2003) Occipito-temporal connections in the human brain. *Brain* 126: 2093–2107.
- [8] Rutherford MA, Cowan FM, Manzur AY, Dubowitz LM, Pennock JM, et al. (1991) MR imaging of anisotropically restricted diffusion in the brain of neonates and infants. *J Comput Assist Tomogr* 15: 188–198.
- [9] Sakuma H, Nomura Y, Takeda K, Tagami T, Nakagawa T, et al. (1991) Adult and neonatal human brain: diffusional anisotropy and myelination with diffusion-weighted MR imaging. *Radiology* 180: 229–233.
- [10] Ment LR, Bada HS, Barnes P, Grant PE, Hirtz D, et al. (2002) Practice parameter: neuroimaging of the neonate – Report of the quality standards subcommittee of the American Academy of Neurology and the Practice Committee of the Child Neurology Society. *Pediatr Radiol* 32: 620–620.
- [11] Hoon AH Jr, Lawrie WT Jr, Melhem ER, Reinhardt EM, Van Zijl PC, et al. (2002) Diffusion tensor imaging of periventricular leukomalacia shows affected sensory cortex white matter pathways. *Neurology* 59: 752–756.
- [12] Lee SK, Mori S, Kim DJ, Kim SY, Kim SY, et al. (2004) Diffusion tensor MR imaging visualizes the altered hemispheric fiber connection in callosal dysgenesis. *AJNR Am J Neuroradiol* 25: 25–28.
- [13] Rollins N (2005) Semilobar holoprosencephaly seen with diffusion tensor imaging and fiber tracking. *AJNR Am J Neuroradiol* 26: 2148–2152.
- [14] Yoo SS, Park HJ, Soul JS, Mamata H, Park HW, et al. (2005) In vivo visualization of white matter fiber tracts of preterm- and term-infant brains with diffusion tensor magnetic resonance imaging. *Invest Radiol* 40: 110–115.
- [15] Zhai GH, Lin WL, Wilber KP, Gerig G, Gilmore JH (2003) Comparisons of regional white matter diffusion in healthy neonates and adults performed with a 3.0-T head-only MR imaging unit. *Radiology* 229: 673–681.
- [16] Inder TE, Warfield SK, Wang H, Hüppi PS, Volpe JJ (2005) Abnormal cerebral structure is present at term in premature infants. *Pediatrics* 115: 286–294.
- [17] Thompson DK, Inder TE, Faggian N, Johnston L, Warfield SK, et al. (2011) Characterization of the corpus callosum in very preterm and full-term infants utilizing MRI. *Neuroimage* 55: 479–490.
- [18] Yu X, Zhang Y, Lasky RE, Datta S, Parikh NA, et al. (2010) Comprehensive brain MRI segmentation in high risk preterm newborns. *PLoS One* 5: e13874.
- [19] van Kooij BJ, de Vries LS, Ball G, van Haastert IC, Benders MJ, et al. (2012) Neonatal tract-based spatial statistics findings and outcome in preterm infants. *AJNR Am J Neuroradiol* 33: 188–194.
- [20] de Bruine FT, van Wezel-Meijler G, Leijser LM, van den Berg-Huysmans AA, van Steenis A, et al. (2011) Tractography of developing white matter of the internal capsule and corpus callosum in very preterm infants. *Eur Radiol* 21: 538–547.
- [21] Parikh NA, Lasky RE, Kennedy KA, McDavid G, Tyson JE (2013) Perinatal factors and regional brain volume abnormalities at term in a cohort of extremely low birth weight infants. *PLoS One* 8: e62804.
- [22] Mori S, Crain BJ, Chacko VP, van Zijl PC (1999) Three-dimensional tracking of axonal projections in the brain by magnetic resonance imaging. *Ann Neurol* 45: 265–269.
- [23] Conturo TE, Lori NF, Cull TS, Akbudak E, Snyder AZ, et al. (1999) Tracking neuronal fiber pathways in the living human brain. *Proc Natl Acad Sci USA* 96: 10422–10427.
- [24] Huang H, Zhang J, van Zijl PC, Mori S (2004) Analysis of noise effects on DTI-based tractography using the brute-force and multi-ROI approach. *Magn Reson Med* 52: 559–565.
- [25] Oishi K, Faria A, van Zijl CM, Mori S (2011) MRI Atlas of Human White Matter. Academic Press. 257 p.
- [26] Wakana S, Caprihan A, Panzenboeck MM, Fallon JH, Perry M, et al. (2007) Reproducibility of quantitative tractography methods applied to cerebral white matter. *Neuroimage* 36: 630–644.
- [27] Pogribna U, Yu X, Burson K, Lasky RE, Narayana PA, et al. (2013) Antecedents of Diffusion Tensor MRI Abnormalities at Term Equivalent Age in a Cohort of Extremely Preterm Infants. *PLoS One*. In Press.
- [28] Pogribna U, Burson K, Lasky RE, Narayana PA, Evans PW, et al. (2013) Role of Diffusion Tensor Imaging (DTI) as an Independent Predictor of Cognitive and Language Development in Extremely Preterm Infants. *AJNR Am J Neuroradiol* In Press.
- [29] Masutani Y, Aoki S, Abe O, Hayashi N, Otomo K (2003) MR diffusion tensor imaging: recent advance and new techniques for diffusion tensor visualization. *Eur J Radiol* 46: 53–66.
- [30] Lee SK, Mori S, Kim DJ, Kim SY, Kim SY, et al. (2004) Diffusion tensor MR imaging visualizes the



altered hemispheric fiber connection in callosal dysgenesis. *AJNR Am J Neuroradiol* 25: 25–28.

- [31] Rollins N (2005) Semilobar holoprosencephaly seen with diffusion tensor imaging and fiber tracking. *AJNR Am J Neuroradiol* 26: 2148–2152.
- [32] Yoo SS, Park HJ, Soul JS, Mamata H, Park HW, et al. (2005) In vivo visualization of white matter fiber tracts of preterm- and term-infant brains with diffusion tensor magnetic resonance imaging. *Invest Radiol* 40: 110–
- [33] Inder TE, Warfield SK, Wang H, Hüppi PS, Volpe JJ (2005) Abnormal cerebral structure is present at term in premature infants. *Pediatrics* 115: 286–294.
- [34] <http://journals.plos.org/plosone/article?id=10.1371/journal.pone.0085807>



The Evolution of 1950s Theater in Miami after the First Major Cuban Exodus

Madison Rolls (Class of 2017)

Major: Classics, Psychology

Principal Investigator/Supervisor: Dr. Lillian Manzor

Department: Modern Languages

Fellowships/Awards/Recognition: Research, Creativity and Innovation Forum 2nd place in Humanities

Senior Thesis: No

This project examines the evolution of theater in Miami during the 1960s after the first major exodus from Cuba. By examining theater spaces in both Havana and Miami, and making connections between spaces and performances, I clarify which aspects of Cuban theater traveled to Miami with the first wave of Cuban exiles. The major research strategy I employ is a quantitative analysis of theater spaces in each city. Data is currently being collected from archives, newspapers and playbills on record in the Cuban Heritage Collection.

Presently, no single, concise collection of information about Cuban theater spaces during the 1950s exists due to the poor nature of Cuba's record keeping system and the general lack of theater ephemera. We know that in the late fifties there occurred the first major exodus from Cuba with the beginning of the new government, and that most of these exiles took refuge in Miami, Florida and the surrounding areas. Research has been done by Dr. Lillian Manzor to map the development of Spanish theater in Miami through information about its performing arts spaces, which began in the 1960s, the same time as Cuban exiles were beginning to build

their new lives in the United States.¹ This led me to believe that there must exist some type of connection between the arrival of the exiles in Miami and its subsequent theater boom. To identify these connections, it became obvious that I would need to begin by understanding the world of theater in Havana directly before the change in government, a concept that has received very little research attention.

Using the archives in the Cuban Heritage Collection of Richter Library, I began by collecting a list of all performing arts spaces in operation during the decade being studied.² After collecting a list of 64 spaces found in texts and performance advertisements, I used both physical copies and digital collections containing theater pamphlets and advertisements to identify as many addresses as possible for the list of spaces.^{3, 4} The addresses were most often found in performance advertisements and pamphlets that listed the location of the performance.⁵ After completing the list of spaces with addresses and any additional information regarding location, I used a Google Fusion table to visually display the data in Havana.

The mapping of data, however, proved to be extremely difficult. Between the period under study and modern day, many of the important roads in Havana have undergone one or multiple name changes, and no maps exist of the city during that time that could be overlaid upon a modern map to mark changes, thereby making it impossible to map the programs to locations based on the information given in the addresses that I had collected. Two methods to resolve the issue



became apparent: mapping could be done by finding which street names have changed and identifying their modern name and subsequently altering the addresses in the list and inputting them into the program, or it could be accomplished by finding the latitude and longitude of each individual location so the program would be able to comprehend the information and place pins accurately. In trying each method of obtaining information, I found that finding latitude and longitude was considerably more time-efficient and effective for the purposes of this project.

After resolving the mapping dilemma, I proceeded to collect a list of spaces that had the same, or similar, names from Dr. Manzor's digital collection of Miami spaces and mapped these as well, with far more ease than the Havana spaces.⁶ I am continuing to work on developing the accuracy of the map and increasing the amount of information available about each space, in the forms of texts and photos. I am also beginning to look at advertisements in both cities to see if similar methods of advertising were employed in each location and how this contributed to the success of the theater spaces.

Thus far, six spaces (e.g. Teatro Martí) have been identified as existing both in Havana and Miami under the same name. It is not yet apparent how the naming of spaces in Miami came about, but there is potential for various reasons. It could be that the theater director for a specific space was exiled, as often was the case for prominent people in the world of theater, and gave the same name to a new theater in Miami. Another possibility is that the theater was

named in honor of an important figure (e.g. Jose Martí) in both locations by different people. Once it is understood by whom, how, and why the theater was named as it was, these connections will become more apparent.

My findings will help to identify and define a large part of the Cuban culture that exists in Miami today and that has been largely overlooked. Future research is needed to make more specific connections between the spaces that I have identified based on a more extensive background research.

References

Websites

[1] L. Manzor (2011, January 1). Retrieved from <http://ctda.library.miami.edu>

Institutions

[2] Cuban Heritage Collection, University of Miami

Books

[3] J. A. González, (2003). *Cronología del teatro dramático habanero, 1936-1960*. Ciudad de La Habana, Cuba: Centro de Investigación y Desarrollo de la Cultura Cubana Juan Marinello.

Digital Collections

[4] María Julia Casanova Papers, Cuban Heritage Collection, University of Miami Libraries, Coral Gables, Florida

[5] Patronato del Teatro Ephemera Collection, Cuban Heritage Collection, University of Miami Libraries, Coral Gables, Florida

[6] Theater Ephemera Collection, Cuban Heritage Collection, University of Miami Libraries, Coral Gables, Florida



Characterization of Palmitic Acid Methyl Ester: A Novel Vasodilator

Stephen Valido and Alexandre do Couto e Silva (Class of 2015)

Major: Microbiology & Immunology

Principal Investigator/Supervisor: Dr. (Kevin) Hung Wen Lin

Department: Neurology

Fellowship/Awards/Recognition:

Characterization of Palmitic Acid Methyl Ester: A Novel Vasodilator, Undergraduate Research, Creativity, and Innovation Forum (RCIF), University of Miami, Coral Gables, Florida, 2015.

Senior Thesis: No

Palmitic acid methyl ester (PAME) is a sixteen-carbon, saturated fatty acid that function as a potent neuroprotector and vasodilator. Its derivative, palmitic acid, is ubiquitous in plants, animals, and microorganisms that does not present with neuroprotection or vasodilatory properties. For this reason, it is important to understand the mechanism in which palmitic acid is converted (methylated form) into PAME. We hypothesize that protein arginine methyl transferases (PRMTs) may be responsible for the methylation of palmitic acid. PAME was first described in the rat superior cervical ganglion (SCG). Our main goal was to identify the possible different types of PRMTs available in the SCG cell bodies.

It was previously discovered by our principle investigator that the release of palmitic acid methyl ester (PAME) from the rat superior cervical ganglion (SCG) induced vasodilation in rabbit aorta upon contact¹. This experiment was done by electrically stimulating the SCG with platinum electrodes at 16 Hz, 300 mA, in a biphasic square wave, thus allowing Krebs' solution to drip from the SCG on to the detector tissue (rabbit aorta)

through the tissue. Krebs' is a physiological solution that prolongs the viability of tissues. After using gas chromatography/mass spectrometry, it was later discovered that PAME was the cause of this vasodilation.

Our main goal as undergraduate researchers was to uncover the possible mechanism(s) in which palmitic acid, which is ubiquitous in many foods we eat (i.e. coconut), is methylated into PAME. We propose that the amino acid, L-arginine is a key molecule involved in the transfer of methyl groups onto palmitic acid (Figure 1).

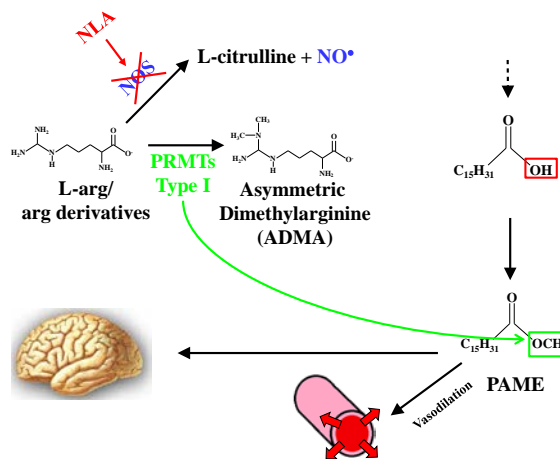


Figure 1. Palmitic Acid Methylation.

As shown in Figure 1, the traditional pathway of L-arginine is the conversion to L-citrulline derived from the Urea cycle via nitric oxide synthase (NOS) forming the by-product nitric oxide (NO). NO is involved in many physiological mechanisms including neuroprotection, vasodilation, neurotransmission, and is a signaling molecule. However, when NOS is inhibited by the presence of Nω-Nitro-L-arginine (NLA) we still observed vasodilation. We



proposed that when the traditional pathway of NO generation is abolished, L-arginine can undergo methylation via protein arginine methyl transferases (PRMTs) and can act as a carrier molecule of methylation directly/indirectly to other species such as palmitic acid. As a result, L-arginine is converted into asymmetric dimethylarginine (ADMA), which can possibly donate methyl groups to palmitic acid, forming PAME.

PRMTs are enzymes that add methyl groups onto arginine residues. There are 10 known types of PRMTs. In order to characterize the presence and relative quantity of PRMTs in the SCG, we performed RNA isolation, reverse transcription polymerase chain reaction of the SCG, and performed gel electrophoresis to visualize possible PRMTs in the SCG. (Figure 2).

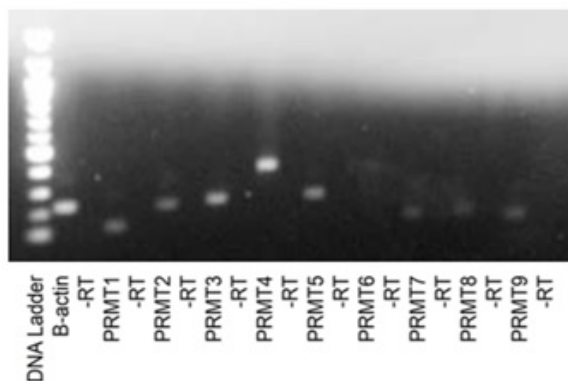


Figure 2. PRMT Expression via Gel Electrophoresis.

After extracting RNA from the SCG, we ran a reverse transcription (RT) to convert the RNA to complementary DNA (cDNA). Once converted, we implemented polymerase chain reaction (PCR) to amplify the cDNA probing for different PRMTs (PRMT 1-9) using primers designed specifically for the

different PRMT isoforms. We used β -actin, a highly conserved protein, as a control due to its large abundance inside our cells. A gel electrophoresis allowed us to separate the DNA by size tagged with ethidium bromide to view its intensity under ultraviolet light (Figure 2). PRMT 4 was the most abundant protein. In general, PRMTs 1-5 showed more abundance than PRMTs 6-9.

Currently, we are working on the same protocol with slight modification: Instead of using a gel electrophoresis to quantify PRMT expression, we are now using quantitative polymerase chain reaction (qPCR) to observe relative mRNA expressions of different PRMTs (Figure 3) in real-time.

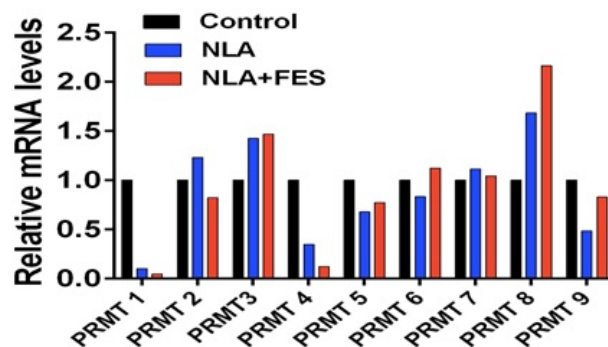


Figure 3. Relative mRNA Expression in qPCR

qPCR allows us to observe relative mRNA in real-time. A cycle is the term used for each time DNA doubles. After a certain amount of cycles, the machine picks up a fluorescent indication and stores it: in general, higher amount of cycles, the higher the mRNA expression. Although we have only performed one trial (n=1) (Figure 3). It is difficult for us to conclude any significant data from our results due to the variability and low number of trials. However, it is



interesting to note that PRMT3, which is located in the cytoplasm, and PRMT8, which is located in the cellular membrane, had higher relative mRNA expression than baseline. In contrast, PRMT1 and PRMT4, both of which are located in the nucleus, had a lower level of mRNA expression.

Our future goals are to characterize the mechanism in which palmitic acid is methylated. We are still in very early stages. The analyses of which PRMTs are responsible for the methylation of L-arginine and palmitic acid will give us a future direction to advancements and studies of the generation of PAME. With these discoveries, we can help formulate new drugs or treatments administered to patients post-stroke promoting recovery.

References

- [1] Lin HW et al., (2008) Endogenous methyl palmitate modulates nicotinic receptor- mediated transmission in the superior cervical ganglion. *Proc. Natl. Acad. Sci. U S A* 105:19525-19530.
- [2] Lin HW et al., (2014) Fatty acid methyl esters and solutol HS 15 confers neuroprotection after focal and global cerebral ischemia. *Transl Stroke Res.* 5:109-117.



The Regulation of Gastrulation in the Anthozoan Cnidarian *Nematostella vectensis*: The Roles of Strabismus and the Cytoskeleton

Régine Vincent (Class of 2015)

Major: Biology & International Studies
Principal Investigator/ Supervisor: Dr. Athula Wikramanayake and Dr. Shalika Kumburegama
Department: Biology
Senior Thesis: No

Morphogenesis is a fundamental component of early development and includes the physical processes that are necessary to form an organism's shape by the re-organization of cells and tissues. Apical constriction (AC) which occurs by the constriction of the apical actin/myosin network forcing the cells to bend inward, is one of these key developmental processes that regulates cell shape change and leads to the formation of critical structures such as the gut in sea urchins and neural tube in humans. Strabismus (Stbm) is a core membrane protein involved in the Wnt/ Planar Cell Polarity cell signaling pathway found to be localized to the apical end of the epithelium at the blastopore is suggested to have a role in the regulation of apical constriction. Knockdown of the Stbm protein inhibits bottle cell formation and primary invagination.¹ Cytochalasin B and Colchicine, two cytoskeletal inhibitors that disrupt actin filaments and microtubules respectively, were used to see if and how the cytoskeleton plays a role in the regulation of Stbm and gastrulation. Results showed in both Cytochalasin B and Colchicine treated embryos, Stbm localization changed and abnormal gastrulation was observed.

Morphogenesis is a fundamental component of early development and includes the physical processes that are

necessary to form an organism's shape by the re-organization of cells and tissues. Apical Constriction (AC) of cells is one example of such a process that regulates cell shape change to internalize cells, and it is a common process during early development in many organisms. AC leads to the formation of critical structures in many species, such as the gut in sea urchins or the forming neural tube in vertebrates. AC occurs by the local activation of myosin, which results in the constriction of the apical actin/myosin network and buckling of the epithelium, forming "bottle cells" and forcing those cells to bend inward. In humans, neural tube defects (NTD) are a commonly seen congenital condition caused by genetic disruptions of genetic pathways regulating AC during early development. Anencephaly, occurring cranially and spina bifida cystica occurring caudally are some of the most severe defects where the neural tissue is not properly closed.²

Studies in many model organisms have shown that AC is frequently regulated by a highly conserved cell signaling pathway called the Wnt/ Planar Cell Polarity (PCP). In *C. elegans* the Wnt signaling pathway was found to regulate gastrulation.³ Studies have shown that multiple mutations in one particular membrane protein in the Wnt/PCP pathway called Strabismus (Stbm) are frequently associated with human NTD. Stbm, a core Wnt/ PCP membrane protein found to be maternally expressed and localized to apical end of the epithelium at the blastopore is required for bottle cell formation and initial gut invagination in *Nematostella vectensis*.¹ This primary



archenteron invagination is necessary for gastrulation to occur. However, the molecular mechanisms used by Stbm to initiate AC, and how the genetic lesions in this gene affect its ability to regulate AC are poorly understood. In order to understand the regulation of AC by Strabismus in the Wnt/PCP signaling pathway we study AC regulation in a simple model system: gastrulation in the Cnidarian *N. vectensis* (Nv), since it undergoes AC during gastrulation. Currently, little is known about the mechanisms that lead to Stbm localization to the apical end of cells at the blastopore, and what additional cellular components work with this protein to mediate AC in *Nematostella*. In this study, we want to test the hypothesis that the cytoskeleton plays a role in regulating Stbm function and gastrulation.

The localization and activation of myosin on apical sides of cells is a common mechanism for the cell shape change required by apical constriction.⁴ We will use Cytochalasin B (irreversible inhibitor) to disrupt the actin filaments and Colchicine to disrupt microtubules and determine if these treatments will disrupt apical constriction and gastrulation. If these drugs have an effect on AC and gastrulation we will determine if there is an effect on Stbm localization and stability.

N. vectensis were cultured in glass bowls and kept in a 17° C incubator. They were fed artemia (brine shrimp) or mussels. Spawning of *Nematostella* requires a 24 hour process of 12 hours in the dark followed by 12 hours in light and the animals spawn 1-2 hours later. Females and males are kept in the

same bowls, so the eggs become fertilized instantly. Eggs were allowed to develop to the blastula stage (4-5 hours post fertilization). Embryos at the blastula stage were collected and de-jellied in a 4% cysteine solution and treated with the drugs for 1 hour. There were 3 treatment groups: one control group of DMSO, one group of Cytochalasin B (10 μ M), and one group of Colchicine (100 μ M). After the allotted time, the embryos were washed with 1/3 seawater and prepared for antibody staining. Antibody staining commenced with fixing the embryos in Memfa fixative for 1 hour and after a post fix on 100% acetone and followed by 3 washes in PBS. The embryos were blocked for 30 minutes to an hour and incubated overnight in the primary antibody Stbm Mid (1:100). The next day they were washed in blocking buffer 3 times and then incubated in secondary antibody (Donkey anti Rabbit 568 1:500) and stained in fluorescein phalloidin (1:500) to localize F actin for 1 hour followed by 3 more washes in blocking buffer and then washed in PBS to prepare to be mounted on slides. The stained embryos were dehydrated in isopropanol, cleared in 1:2 Benzyl Alcohol: Benzyl Benzoate solution and examined using a Leica SP5 scanning confocal microscope.

Antibody staining with Stbm Mid primary antibody (1:100), D α R 568 secondary antibody (1:500) and phalloidin (1:500) showed the following results In the DMSO control, Stbm staining was localized to the apical end of the animal plate



epithelium, which is the expected result for the control. In the Cytochalasin B treated group, the actin skeleton was disrupted, which was expected. Stbm staining was still localized to the apical side of the cells but also the staining appeared to be observed all throughout the cell. Furthermore, the staining did not appear to be that bright, suggesting that the Stbm protein may have been degraded. In the Colchicine treated group, Stbm staining seems to move off the membrane and become localized to a subapical region of cells. While the staining appears to be nuclear, this has to be validated by double staining using nuclear dye. Staining of embryos were performed to see the phenotype of the treatment group. In embryos stained with Propidium Iodide and Phalloidin gastrulation occurs normally in DMSO control but showed to be abnormal and cytoskeleton is disrupted in Cytochalasin B treated embryos. For colchicine treated embryos stained with Propidium Iodide and Phalloidin multiple layers are observed in embryos.

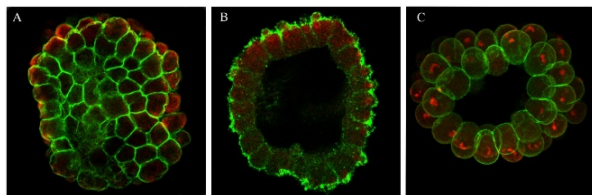


Figure 1. Embryos stained with Stbm Mid primary antibody, DaR 568 secondary antibody and phalloidin (A) In the DMSO control, Stbm staining was localized to the apical end of the animal plate epithelium. (B) In the Cytochalasin B treated group, the actin skeleton was disrupted. Stbm staining was still localized to the apical side of the cells but also the staining appeared to be observed all throughout the cell. (C) In the Colchicine treated group, Stbm staining seems to move off the membrane and become localized to a subapical region of cells

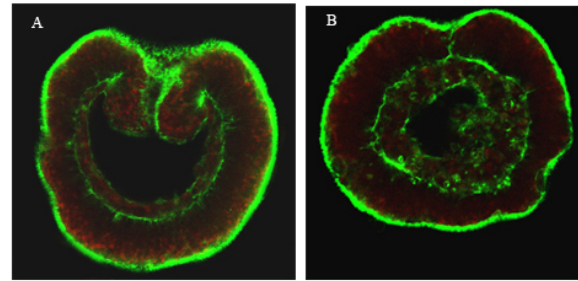


Figure 2. Embryos stained with Propidium Iodide and Phalloidin (A) Gastrulation occurs normally in DMSO control (B) Gastrulation is abnormal and cytoskeleton is disrupted in Cytochalasin B

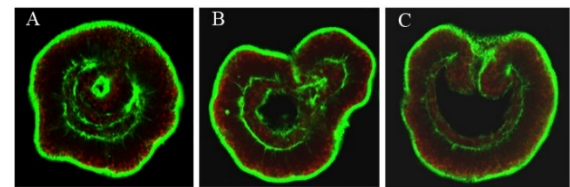


Figure 3. Embryos stained with Propidium Iodide, (A) and Phalloidin, (B) multiple layers are observed in embryos, (C) gastrulation occurs normally in control

Three main results were observed: first, disrupting the cytoskeleton affects Stbm localization, second, abnormal gastrulation in Cytochalasin B treated embryos and finally multiple gastrulation sites occurs in Colchicine treated embryos. We would like to further examine the relationship between the cytoskeleton Stbm localization and gastrulation. We want to make sure we are not just completely destroying the embryos by adding these cytoskeletal inhibitors but observing the relationship and effects. Next, we might try treating the embryos for different amounts of time and seeing the effects. Western blot analysis will be performed to quantify results.



References

- [1] S. Kumburegama, N. Wijesena, R. Xu, A. H. Wikramanayake (2011). Strabismus- mediated primary archenteron invagination is uncoupled from Wnt/ β -catenin-dependent endoderm cell fate specification in *Nematostella vectensis* (Anthozoa, Cnidaria): Implication for the evolution of gastrulation
- [2] T. W. Sadler (2005) Embryology of Neural Tube Development
- [3] J-Y Lee, D. J. Marston, T. Walston, J. Hardin, A. Halberstadt, B. Goldstein (2006) Wnt/ Frizzled Signaling Controls *C. elegans* Gastrulation by Activating Actomyosin Contractility
- [4] J. M. Sawyer, J. R. Harrell, G. Shemer, J. Sullivan-Brown, M. Roh-Johnson, B. Goldstein (2010) Developmental Biology 341 5-19 Apical constriction: A cell shape change that can drive morphogenesis